International Journal of Heat and Mass Transfer 52 (2009) 3481–3489

Contents lists available at ScienceDirect

International Journal of Heat and Mass Transfer

journal homepage: www.elsevier.com/locate/ijhmt

Non-linear analyses of temperature oscillations in a closed-loop pulsating heat pipe

Jian Qu [a], Huiying Wu [a,*], Ping Cheng [a], Xiong Wang [b]

[a] Key Laboratory for Power Machinery and Engineering of Ministry of Education, School of Mechanical and Power Engineering, Shanghai Jiaotong University, Shanghai 200240, PR China

[b] Department of Mathematics, Shanghai Jiaotong University, Shanghai 200240, PR China

ARTICLE INFO

Article history:
Received 5 November 2008
Received in revised form 7 March 2009
Accepted 7 March 2009
Available online 17 April 2009

Keywords:
Pulsating heat pipe
Temperature oscillation
Non-linear dynamics
Chaotic behavior

ABSTRACT

In this paper, the chaotic behavior of wall temperature oscillations in a closed-loop pulsating heat pipe was investigated using non-linear analyses on temperature data. The tested heat pipe, consisting of 5 turns, was made of copper capillary tube and had an internal diameter of 2 mm. Ethanol was selected as the working fluid with filling ratios (FR) of 30%, 50% and 70%. Wall temperature fluctuations were recorded under three different heating power inputs of 37, 60, and 87 W. Various methods, including pseudo-phase-plane trajectories, correlation dimensions (D_E), Lyapunov exponents, and recurrence plots, were used to analyze the non-linear dynamics characteristics of temperature oscillation data. Three types of attractors were identified under different power inputs. All of the calculated positive largest Lyapunov exponents were found to be less than 0.1, demonstrating the weak chaos characteristics of the pulsating heat pipe. The increase of the power input augments the correlation dimensions and contributes to the improvement of the thermal performance of the pulsating heat pipe. For each power input, the correlation dimensions have the trend of $D_{E,FR=50\%} > D_{E,FR=70\%} > D_{E,FR=30\%}$, and the best thermal performance was obtained at 50% filling ratio. At least four independent variables are required in order to describe the heat transfer characteristics of a PHP. The average time of the temperature oscillation stability loss, i.e., the inverse of the largest Lyapunov exponent, decreases as the power input increases. In the recurrence plots, chaotic states were observed. The Recurrence Quantification Analysis indicates larger values of the order-2 Renyi entropies K_2 at the evaporation section than at the condensation section. Moreover, the trend that $K_{2,Q=87W} > K_{2,Q=60W} > K_{2,Q=37W}$ at each filling ratio both for T_{e4} and T_{c4} collaborating with the positive, finite largest Lyapunov exponent gives a hint of the maximum entropy self-organization process of the temperature oscillations with the increase of power input.

1. Introduction

The pulsating heat pipe (PHP), proposed and patented by Akachi [1], is a new member of the wickless heat pipes. Due to its excellent features, such as high thermal performance, rapid response to high heat load, simple design and low cost, PHP has been considered as one of the promising technologies for electronic cooling, heat exchanger, cell cryopreservation, etc.

A typical PHP consists of a meandering looped capillary tube with multiple turns. The internal diameter of the tube is restricted by a Bond number less than 2 [2], which is a fundamental requisition for PHP operation. Fig. 1 illustrates a closed-loop pulsating heat pipe, which can be fabricated by evacuating the capillary tube, and then partially filled with a phase-change working fluid. It will distribute itself naturally in the form of liquid slugs and vapor plugs inside the capillary tube. Heat is transferred from the evaporation section to the condensation section of the heat pipe through pulsating action of the liquid–vapor/bubble–slug system, which is mainly caused by the thermally induced pressure/density pulsations inside the device [3]. Usually, an adiabatic zone exists between the evaporation and condensation sections.

A number of researchers have conducted experimental investigations on PHPs, and the results indicated that the heat transfer capability of PHPs mainly depends on the working fluids, evaporation/condensation lengths, inner diameters, turn numbers, etc [4]. In addition to the experimental research, various mathematical models have also been developed in recent years to predict the oscillating motion and heat transfer performance of the PHPs. Using a Lagarangian approach, Wong et al. [5] simplified the PHP operating mechanism with a spring-mass-damper system under the adiabatic condition, and predicted the kinematics behaviors of liquid slugs and vapor plugs. By assuming a meandering PHP to be an unfolded straight tube, Shfii et al. [6] and Zhang et al. [7] solved the governing equations of mass, momentum and energy to simulate behaviors of liquid slugs and vapor plugs in both closed-loop PHP and closed-end PHP. They concluded that the number of vapor plug eventually was reduced to equal the number

* Corresponding author. Tel.: +86 21 34205299; fax: +86 21 34206337.
E-mail address: whysrj@sjtu.edu.cn (H. Wu).

0017-9310/$ - see front matter © 2009 Elsevier Ltd. All rights reserved.
doi:10.1016/j.ijheatmasstransfer.2009.03.012

Nomenclature

C	correlation integral
D_E	correlation dimension
FR	filling ratio
Ja	Jakob number
K	Kolmogorov–Sinai entropy
K_2	order-2 Renyi entropy
Ka	Karman number
l	length of diagonal line segments
m	embedding dimension
N	number of turns; number of embedding points
P	pressure (N/m^2)
Pr	Prandtl number
q	heat flux (W/m^2)
Q	heating power input (W)
R	thermal resistance (°C/W); recurrence function
S	average diverging rate
t	time (s); time span
T	temperature (°C)
x	point in embedding space
x	vector in embedding space

Greek symbols

β	tilt angle (°)
ε	radius; threshold distance
λ	largest Lyapunov exponent (bit/ s)
ρ	initial neighborhood size
σ	standard deviation
τ	time delay
Θ	Heaviside step function

Subscripts

sat	saturation state
e1, e2, e3, e4, e5	temperature test point at the evaporation section
c1, c2, c3, c4, c5	temperature test point at the condensation section
i, j	the ith and jth point in phase space
n	the nth point in phase space; point number
0	initial conditions

of evaporation turns. Moreover, the sensible heat exchange was found to play a predominant role in the total heat transfer in PHP. With the aid of a visualization study, Sakulchangsatjatai et al. [8] proposed a mathematical model that could efficiently represent the behavior of the working fluid in a close-end PHP in an inclined position. The simulation results for the number of vapor plugs, void fraction in the evaporation section and the heat transfer rate were found in good agreement with the visualization results. Khandekar et al. [4] developed a semi-empirical formulation for predicting the heat flux of a closed-loop PHP. Qu and Ma [9] presented a mathematical model to describe the startup of a PHP. They found that the inner wall surface condition, evaporation in the hot section, superheat, bubble growth, and the amount of vapor bubble trapped in cavities affected the startup of a PHP. Although extensive studies have been carried out in the past decade, certain key aspects of the PHP remain poorly understood, and some analytical results obtained by different investigators are even contradictory to the experimental data.

Since bubble nucleation and collapse, bubble expansion and shrinkage, pumping action, pressure/temperature perturbations, two-phase flow instabilities coexist in a PHP, a mathematical model which accounts for these physical phenomena in a PHP is very complicated and non-linear in nature. Although much experimental and theoretical work has been performed on the PHP, limited non-linear analyses work has been carried out only recently [10–12]. By calculating Lyapunov exponents, Dobson [10] showed that his theoretical model could reflect the chaotic behavior of the fluid in an open PHP. Maezawa et al. [11] performed a non-linear dynamics analysis of temperature fluctuations in a close-end PHP adiabatic section, and suggested the existence of chaos in a PHP. Xu and Zhang [12] applied PSD (power spectral density), a non-linear tool, to analyze steady temperature oscillations of a three-turn closed-loop PHP. A couple of dominant characteristic frequencies were found at high power input and indicated the quasi-periodic behavior of the oscillating flow, which was inconsistent with the chaotic behavior in the open PHP [10] and the closed-end PHP [11].

In this paper, we will extend the work done by Dobson [10], Maezawa et al. [11] and Xu and Zhang [12] by performing a more comprehensive study on temperature oscillations of a closed-loop PHP using non-linear analyses. The non-linear analyses are based on reliable records of the time series of wall temperatures, which were collected at the evaporation and condensation sections in our closed-loop PHP. The results of this investigation will provide a better understanding of the fluid flow and heat transfer phenomena occurring in a PHP.

2. Experimental setup and measurements

2.1. Experimental setup

Fig. 2 illustrates the experimental setup, consisting of a closed-loop PHP assembly, a multi-channel data acquisition system, a DC

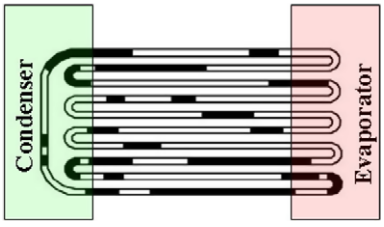

Fig. 1. The configuration of a closed-loop pulsating heat pipe.

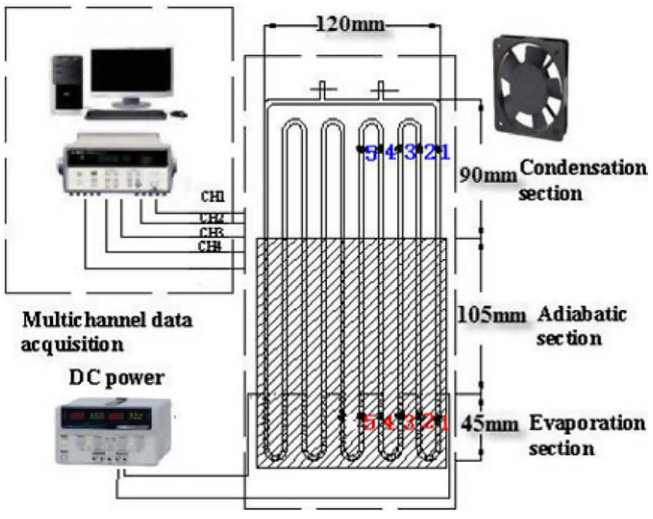

Fig. 2. Experimental setup of the PHP.

power supply unit (GW, GPR-3060D) and a fan cooling system. The PHP was fabricated by bending a copper capillary tube with the inner diameter of 2 mm and outer diameter of 3 mm. It had 5 turns and the inner radius of each turn was 6 mm. The PHP, consisting of evaporation, adiabatic and condensation sections (with 45, 105 and 90 mm in length, respectively), was inclined at the angle of 70° in this experiment. Heat was supplied to the evaporation section by wrapping the Ni–Cr heating wire with a diameter of 0.3 mm on the outer surface of the capillary tube, and was dissipated from the condensation section by forced air convection driven by a fan (220 V/AC) at an ambient temperature of 20 °C. Both the evaporation and adiabatic sections were well thermally insulated by the insulation materials, and the heat loss from these two sections to the ambience was estimated to be less than 5% of the total heating power input.

The Agilent 34970A data acquisition system, including a multi-channel data logger and a computer, was used to record the experimental data. Ten thermocouples with a diameter of 0.1 mm (OMEGA T-type with ± 0.1 °C accuracy) were mounted on the wall of the PHP. As illustrated in Fig. 2, five thermocouples (T_{e1}, T_{e2}, T_{e3}, T_{e4}, T_{e5}) were placed in the evaporation section and the other five thermocouples (T_{c1}, T_{c2}, T_{c3}, T_{c4}, T_{c5}) were placed in the condensation section. Due to the high thermal conductivity and small wall thickness (0.5 mm) of the copper tube, the temperature difference between the inner surface and outer surface was negligible. Therefore, the temperature measured by the thermocouples could be approximately regarded as the fluid temperature in the PHP tube. Ethanol was selected as the working fluid because of its low latent heat and high $(dP/dT)_{sat}$ [3]. Three different filling ratios, 30%, 50% and 70%, were selected for this experiment. The heating power input was stepwise increased during the experiment, and temperature data at the evaporation and condensation sections were recorded after the system had reached a steady state condition. When recoding temperature oscillations data, only two data channels for T_{e4} (at the evaporation section) and T_{c4} (at the condensation section) are open to guarantee the fast recording speeds, while during measuring the overall PHP thermal resistances R (defined as the ratio of the average temperature difference between the evaporation and condensation sections to the power input), all ten data channels for T_{e1}, T_{e2}, T_{e3}, T_{e4}, T_{e5} and T_{c1}, T_{c2}, T_{c3}, T_{c4}, T_{c5} (shown in Fig. 2) were open.

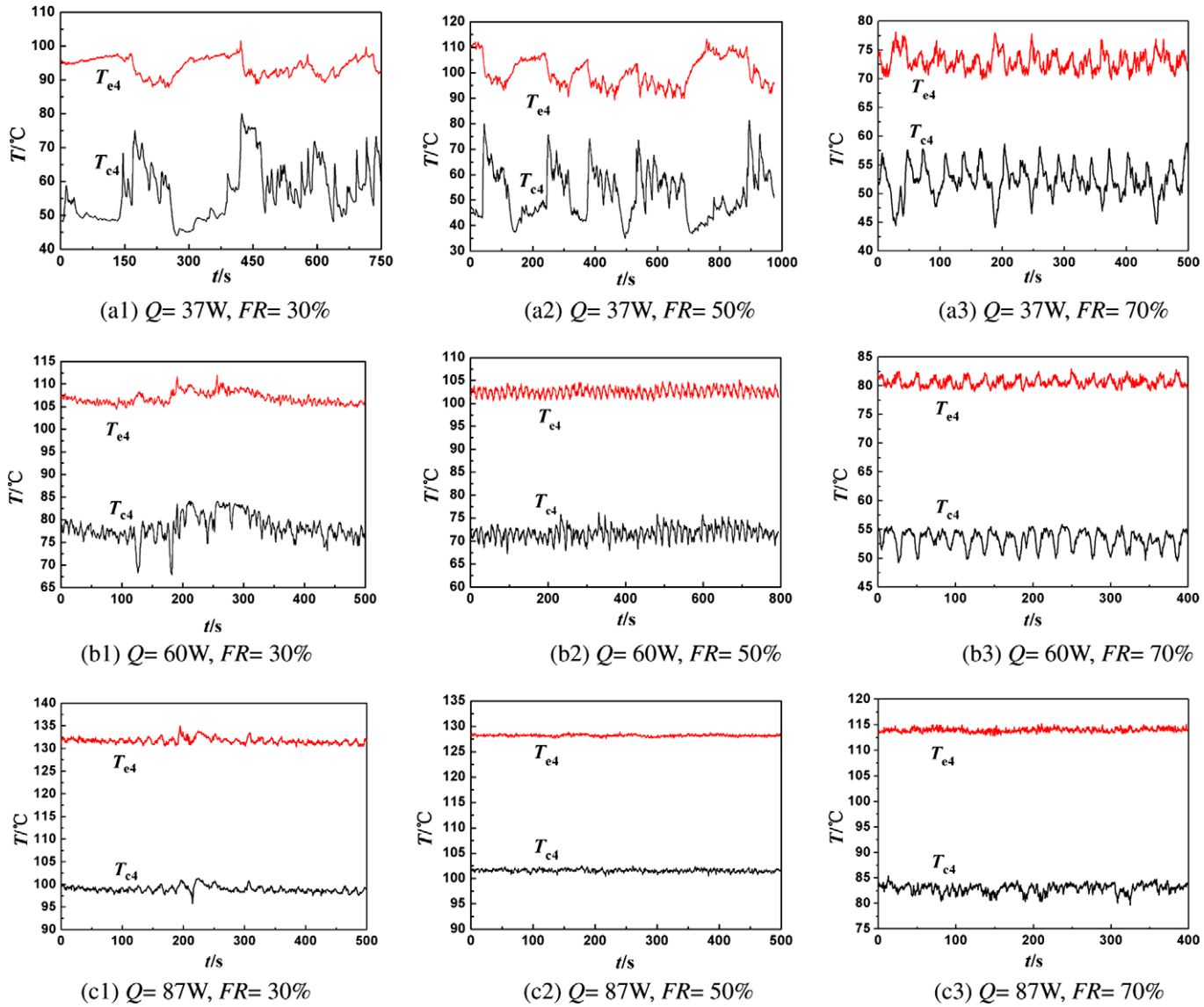

Fig. 3. Temperature oscillations of T_{e4} and T_{c4} in the PHP at different filling ratios (30%, 50%, 70%) and power inputs (37, 60, 87 W).

2.2. Temperature oscillations in the closed-loop PHP

Vapor-plug/liquid-slug flow is the dominating two-phase flow in a PHP. Thus, the inner wall surface of the PHP in operation was flushed by the vapor plug and liquid slug alternatively, which accounted for the temperature perturbation [12]. Fig. 3 shows the temperature oscillations of T_{e4} (evaporation section) and T_{c4} (condensation section) at filling ratios of 30%, 50%, and 70% under three different power inputs of 37 W (low power input), 60 W (medium power input), and 87 W (high power input), respectively. At each power input, temperatures were recorded after the steady state was reached. As can be seen from Fig. 3, the average oscillation cycle time (AOCT) and average oscillation amplitude (AOA) of T_{e4} and T_{c4} varied with power inputs significantly. At low power input of $Q = 37$ W, owing to smaller pressure instability between the tubes, the velocity of the working fluid in the capillary tube is slower. Under such condition, the flow is characterized by "movement–stationary–movement", and the bulk circulation rarely occurred [13]. Thus, the temperature fluctuates with large amplitude at $Q = 37$ W as shown in Fig. 3(a1), (a2) and (a3). At medium power input of $Q = 60$ W, "movement–stationary–movement" flow gives way to the bulk circulation accompanied by occasional local flow direction switching. The continuous fast movement of the working fluid reduces the AOA and AOCT of T_{e4} and T_{c4} as shown in Fig. 3(b1), (b2) and (b3) compared with those in Fig. 3(a1), (a2) and (a3). When the high power input of 87 W was applied, the bulk circulation velocity increased further, and consequently the AOA of T_{e4} and T_{c4} were the smallest as shown in Fig. 3(c1), (c2) and (c3). In the following section, the non-linear dynamic theory will be used to analyze temperature oscillations in evaporation and condensation sections in order to investigate the chaotic behavior of the PHP.

3. Non-linear dynamic analyses and discussions

The non-linear time series analysis is a widely-used method for the study of complicated dynamical systems. Various non-linear analytical tools, including pseudo-phase-plane trajectories, correlation dimensions, Lyapunov exponents, and recurrence plots, are now employed to analyze the temperature time series at evaporation and condensation sections presented in Fig. 3.

3.1. Pseudo-phase-plane trajectories

Behaviors of a chaotic system can be analyzed based on the trajectories of attractors in the phase space [14–16]. For a complex system, there are usually a large number of variables that can not be measured completely. However, most dynamical systems involve only a small number of important variables. Therefore, the study can often be restricted to a relatively low-dimensional phase space that only includes the most important variables. Such a phase space is usually called embedding space (i.e., pseudo-phase-plane), which can be reconstructed with the time-delay method. Vector time series of temperature in an embedding space are formed from time-delayed values of the scalar measurements [16]:

$$T_n = \{T(t_n), T(t_n + \tau), T(t_n + 2\tau), \cdots, T[t_n + (m-1)\tau)]\} \quad (1)$$

where the number m is called the embedding dimension, and the time τ is referred to as the delay or lag.

If the sequence $\{T_n\}$ does indeed consist of scalar measurements of the state of a dynamical system, the time delay embedding provides a one-to-one image of the original trajectories, i.e., the topological properties are preserved. Therefore, the accuracy of the time delay τ is fundamentally important for the attractor reconstruction, as well as for the computation of other invariant parameters characterizing system behavior, such as correlation dimensions and the largest Lyapunov exponents. To estimate the "optimal" embedding dimension, the method of false nearest neighbors or Cao's method [17] is applied. The most frequently applied methods for estimation of τ are based on the autocorrelation function or on the mutual information [18], and the latter is applied herein.

For the visualization of the pseudo-phase-plane trajectories of attractors, the values of $m = 2$ and $m = 3$ are often used [14–16]. Fig. 4 presents the reconstructed 3D attractors from the temperature time series of T_{e4} and T_{c4} for FR = 50% corresponding to Fig. 3(a2), (b2) and (c2). Although we do not assume nor claim that the attractors are deterministic or even chaotic, the structure of the 3D attractors in Fig. 4 is worthy of consideration: at low power input of $Q = 37$ W, the attractors shown in Fig. 4(a) and (b) are in slim and elongated patterns, a hint of a low-dimension characteristic of the temperature oscillation. At medium power input of $Q = 60$ W, the attractors as shown in Fig. 4(c) and (d) are more complex, e.g., a torus-like structure is observed. At high power input of $Q = 87$ W, the attractors as shown in Fig. 4(e) and (f) are more complex, which evidences a high-dimension characteristic of the temperature oscillation. For other temperature oscillations at FR = 30% and 70% in Fig. 3, the similar 3D temperature pseudo-phase-plane trajectories of attractors as shown in Fig. 4 can be constructed. In order to prove that these attractors are strange attractors of chaotic features, the correlation dimensions are calculated next.

3.2. Correlation dimensions

Strange attractors with non-integer fractal dimension are typical feature of a chaotic system. There are many types of definitions of fractal dimensions, for which the correlation dimension is the most widely-used method to estimate the fractal dimension of an attractor. The power-law relation between the correlation integral of an attractor and the neighborhood radius of the analysis hyper-sphere can be used to provide an estimate of the correlation dimension D_E [15]:

$$D_E = \lim_{\varepsilon \to 0} \frac{\ln C(\varepsilon, \tau, m)}{\ln \varepsilon} \quad (2)$$

where $C(\varepsilon, \tau, m)$ is the correlation integral which is defined by:

$$C(\varepsilon, \tau, m) = \frac{1}{N(N-1)} \sum_{i=1}^{N} \sum_{\substack{j=1 \\ j \neq i}}^{N} \Theta(\varepsilon - \|x_i - x_j\|) \quad (3)$$

where x_i are the points on the attractor, and N is the number of embedding points in phase space. The correlation integral is essentially a measure of the number of points within a neighborhood of radius ε, average over the entire attractor. $\|.\|$ presents a norm (e.g., the Euclidean norm) and $\Theta(\cdot)$ is the Heaviside step function, which satisfies: $\Theta(x) = 1$ for $x > 0$ and $\Theta(x) = 0$ for $x \leqslant 0$.

Usually, the correlation dimension D_E is determined by calculating the value of the slope of the fitting line crossing a middle scale region of the $\ln C(\varepsilon, \tau, m)$ versus $\ln \varepsilon$ curve [15]. When the value of N in the denominator of Eq. (3) is significantly large, D_E, for a chaotic system, will converge with the increase of the embedding dimension m. In contrast, D_E of a noise increases with the increase of the embedding dimension m. Fig. 5(a) shows the seven correlation integral curves of T_{c4} at 50% filling ratio and 37 W power input for $m = 15, 20, 22, \ldots, 30$, respectively. The dashed line in Fig. 5(a) is the fitting line for embedding dimension of 30 ($m = 30$). At the filling ratio of 50% and power input of 37 W, the correlation dimension for T_{c4} ($m = 30$) is 2.16. Other correlation dimensions for T_{e4} and T_{c4} at different conditions are listed in Table 1. The slopes of

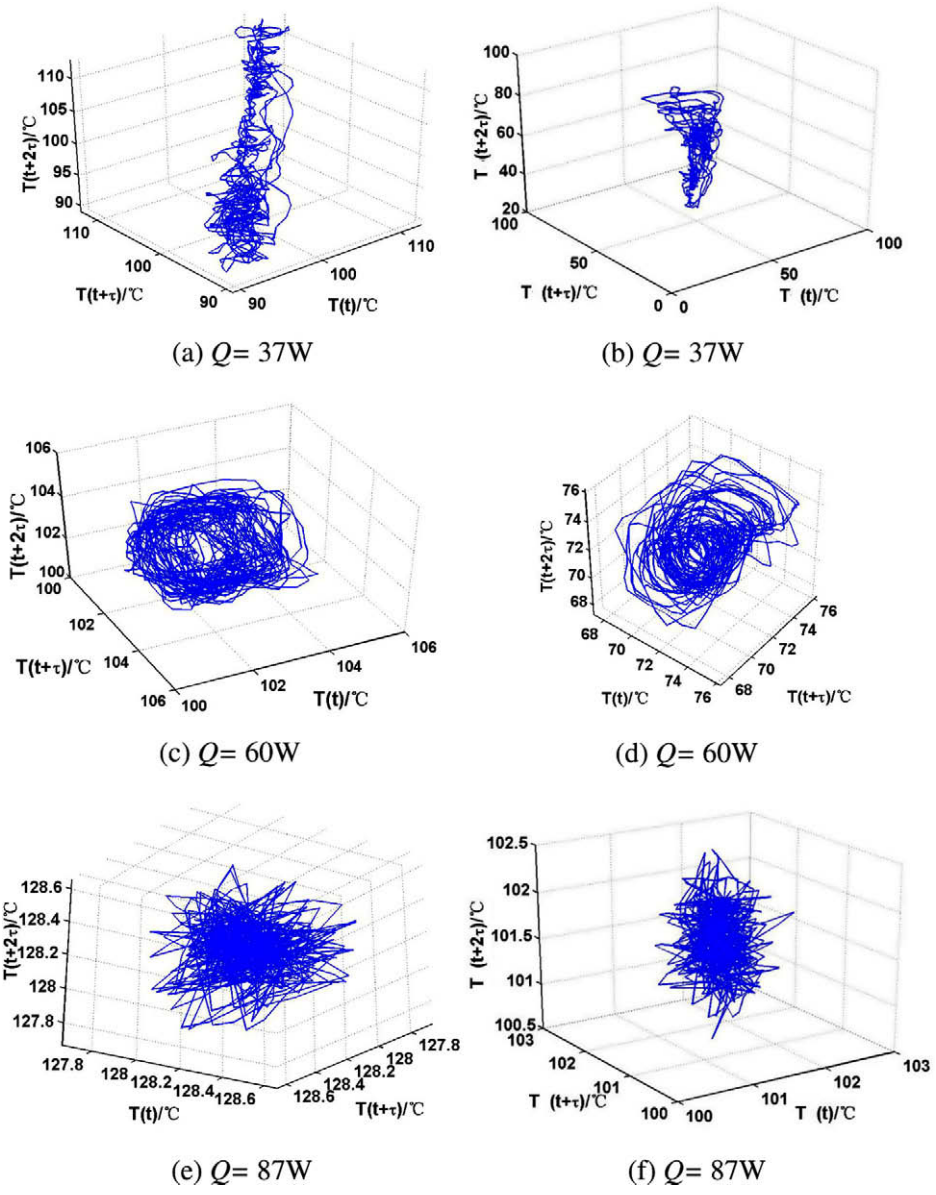

Fig. 4. Reconstructed 3-D attractors of T_{e4} (left) and T_{c4} (right) for FR = 50% at different power inputs.

ln $C(\varepsilon, \tau, m)$ versus ln ε curves of T_{c4} under power inputs Q = 37, 60, 87 W at 50% filling ratio are presented in Fig. 5(b). It is shown that with the increase of m, D_E increases initially, and then approaches a constant value when m is significantly large at a given power input. The non-integer correlation dimension listed in Table 1 and the value of D_E approaching a constant in Fig. 5(b) indicates the

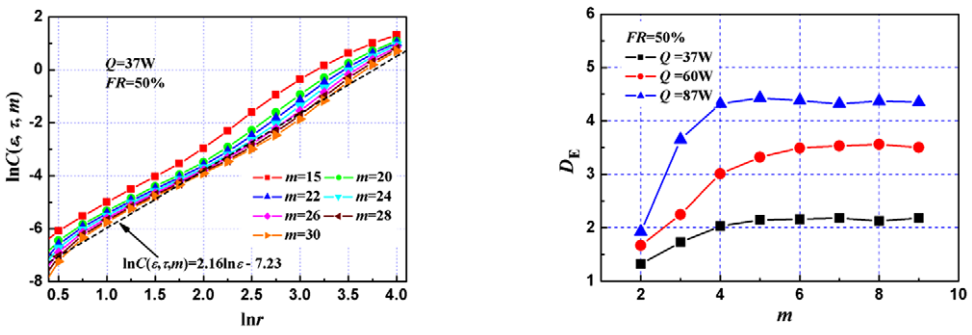

Fig. 5. Correlation dimensions of T_{c4} at 50% filling ratio.

Table 1
Results of non-linear analysis for temperature oscillations and thermal resistances of PHP.

Filling ratio, FR	Power input, Q	Test point	Correlation dimension, D_E	Largest Lyapunov exponent, λ	Thermal resistance, R
30%	37	T_{e4}	2.35	0.037	0.909
		T_{c4}	2.11	0.029	
	60	T_{e4}	3.76	0.052	0.52
		T_{c4}	3.16	0.044	
	87	T_{e4}	3.89	0.060	0.38
		T_{c4}	3.63	0.063	
50%	37	T_{e4}	2.62	0.039	0.63
		T_{c4}	2.16	0.031	
	60	T_{e4}	4.52	0.044	0.49
		T_{c4}	3.49	0.036	
	87	T_{e4}	4.77	0.065	0.32
		T_{c4}	4.34	0.061	
70%	37	T_{e4}	2.49	0.023	0.71
		T_{c4}	2.27	0.017	
	60	T_{e4}	4.2	0.042	0.47
		T_{c4}	3.23	0.032	
	87	T_{e4}	4.52	0.057	0.35
		T_{c4}	4.13	0.052	

deterministic chaos rather than noise or periodic/quasi-periodic characteristics of the PHP. Therefore, the attractors in Fig. 4 are strange attractors, which prove the chaos characteristics of temperature oscillations.

The value of correlation dimension D_E represents the complexity of a system. When the power input is increased from 37 to 87 W at the same filling ratio (shown in Table 1), the correlation dimensions of T_{e4} or T_{c4} increases either, indicating the complexity of the PHP system increase, which is consistent with the discussions on the attractors at different power inputs in Section 3.1. Meanwhile, as the power input increases, the thermal resistance (listed in Table 1) decreases, i.e., the thermal performance of PHP is improved. Furthermore, at the same power input and the same filling ratio, the correlation dimension of T_{e4} at the evaporation section is larger than that of T_{c4} at the condensation section, implying that temperature oscillations in the evaporation section is more complex. This may be attributed to the "pumping" role that the evaporation section plays in a PHP. With the increase of the filling ratio, the correlation dimensions of T_{e4} or T_{c4} at each same power input have a trend of $D_{E,FR=50\%} > D_{E,FR=70\%} > D_{E,FR=30\%}$ except for T_{c4} at $Q = 37$ W between FR = 50% and FR = 70%, and accordingly, the related thermal resistances at each same power input have a trend of $R_{FR=50\%} < R_{FR=70\%} < R_{FR=30\%}$ except at the condition of $Q = 60$ W between FR = 50% and FR = 70%. Therefore, the enhancement of the complexity of the PHP system, i.e., the increase of the correlation dimension from a low-value to a higher value, leads to the decrease of thermal resistance and the increase of thermal performance of a PHP.

A more complex system has a higher correlation dimension, which means that more independent variables are needed to describe its dynamic behavior. The number of independent variables controlling the behavior of the system is a smallest integer number greater than the correlation dimension. At lowest power input of Q = 37 W (shown in Table 1), the values of all correlation dimensions of T_{e4} and T_{c4} are between 2 and 3. However, the values of the correlation dimensions are between 3 and 5 for higher power inputs (60 and 87 W). Therefore, the PHP under higher power inputs is more complex, which require more independent variables to describe its oscillation characteristics. A PHP with small AOA is desirable because constant temperature is a favorable requirement of a heat pipe. Hence, the PHP operating under the medium and high power inputs with relatively smooth temperature perturbations is worthy of consideration, and thus the number of independent variables to describe the PHP operation under such conditions is at least four. Note that the semi-empirical correlation of heat transfer in a PHP at a fixed filling ratio of 50% given by Khandekar et al. [4] is:

$$q = 0.54[\exp(\beta)]^{0.48} Ka^{0.47} Pr_{liq}^{0.27} Ja^{1.43} N^{-0.27} \quad (4)$$

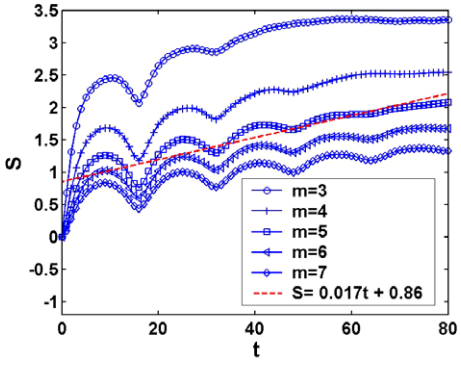

Fig. 6. The largest Lyapunov exponent for T_{c4} for different m (at $Q = 37$ W, FR = 70%).

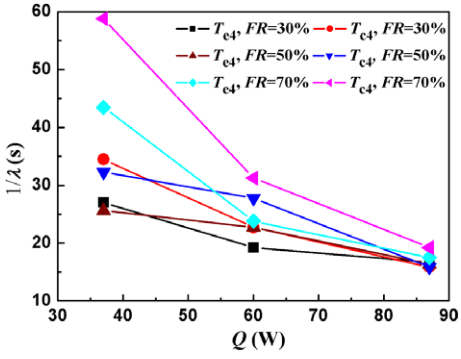

Fig. 7. $1/\lambda$ of T_{e4} and T_{c4} versus Q at different filling ratios.

where q is the heat flux with β, N, Ka, Pr_{liq}, and Ja representing the tilt angle, the turn number, the Karman number, the liquid Prandtl number, and the Jakob number, respectively. For a more generalized case, the effect of filling ratio (FR) is required. Consequently, the heat flux is determined by six independent variables β, N, Ka, Pr_{liq}, Ja and FR. For a given PHP with fixed tilt angle β and turn number N, the latter four parameters are needed to describe the thermal performance of the PHP. This is consistent with the correlation dimensions analysis result we have obtained above, that the number of independent variables to describe the PHP operation is at least four.

3.3. Lyapunov exponent

The Lyapunov exponent is a measure of the sensitivity to initial conditions, the primary characteristic of a chaotic system. Actually there is a whole spectrum of Lyapunov exponents due to different orientations of initial separation trajectories. It is common to just refer to the largest one, i.e., the largest Lyapunov exponent λ, because it determines the predictability of a dynamical system. The value of the largest Lyapunov exponent λ is negative for a fixed stable point and zero for a periodic or quasi-periodic behavior. On the other hand, the value of λ is positive with finite and infinite values

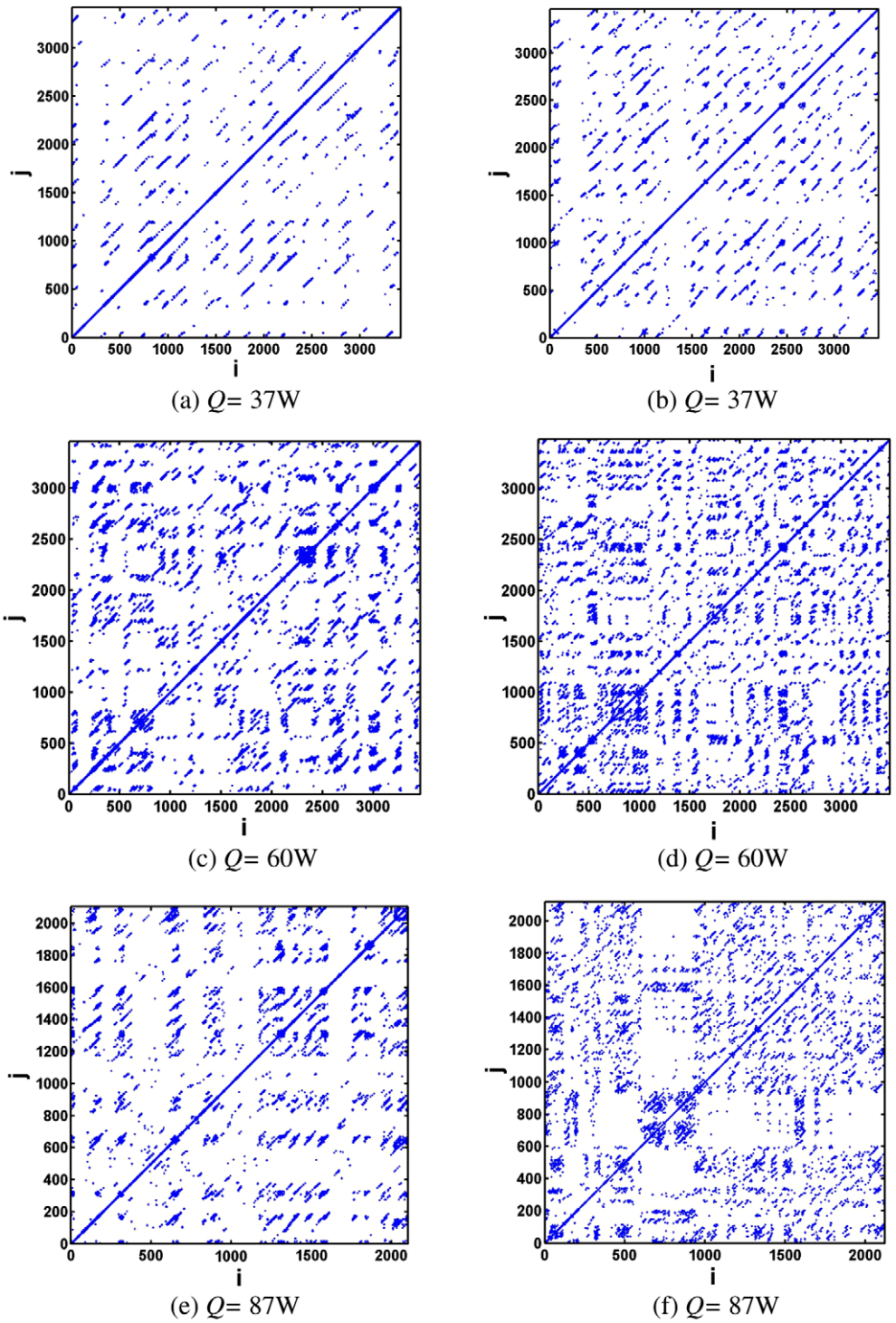

Fig. 8. Recurrence plots of T_{e4} (left) and T_{c4} (right) for FR = 70% at different power inputs ($\varepsilon = 0.5\sigma$).

for a chaotic and random noise behavior. The approach proposed by Wolf et al. [19] has been commonly used to determine the largest Lyapunov exponent. Recently, Kantz [20] developed a more accurate approach to determine the largest Lyapunov exponent. If a very close return $x_{n'}$ to a previously visited initial point x_n in embedding space is observed, then one can consider the distance $\Delta_0 = x_n - x_{n'}$ as a small perturbation, which grow exponentially in time. Its future can be read from the time series $\Delta_l = x_{n+l} - x_{n'+l}$. If one finds $|\Delta_l| \approx \Delta_0 e^{\lambda l}$, then the largest Lyapunov exponent can be obtained, and the nature of oscillation can be determined. A more useful formula is given by Kantz and Schreiber [21] as:

$$S(\rho, m, t) = \left\langle \ln\left(\frac{1}{|u_n|}\sum_{x_{n'}\in u_n} |x_{n+t} - x_{n'+t}|\right)\right\rangle_n \quad (5)$$

where $S(\rho, m, t)$ is the average diverging rate, u_n is the neighborhood with diameter ρ. If the value of $S(\rho, m, t)$ exhibits a linear increase with identical slope for all m larger than some m_0 and for a reasonable range of ρ, then the slope can be taken as an estimate of the largest Lyapunov exponent. Fig. 6 shows the curves of S versus t (i.e., time span containing the deterministic fluctuations) for T_{c4} at Q = 37 W and FR = 70%, at five values of m (m = 3–7). As can be seen from Fig. 6 that the average slope of the curves S is independent of the embedding dimension m when m is larger than 5. Using linear regression for the curve of m = 5, we can determine the value of the largest Lyapunov exponent λ = 0.017. The largest Lyapunov exponents for T_{e4} and T_{c4} at other conditions are also listed in Table 1. The positive values of λ provide the evidence of chaotic motion of the working fluid in the PHP. Generally, larger positive λ means stronger chaotic level. The values of estimated largest Lyapunov exponent shown in Table 1 exhibit an increasing tendency as power input increases for each filling ratio, demonstrating the increase of the chaotic level of the oscillations as power input increases. It is also shown that the values of all largest Lyapunov exponents listed in Table 1 are less than 0.1, indicating the weak chaotic characteristic rather than the noise and quasi-periodic behavior of the PHP.

The inverse of largest Lyapunov exponent, or $1/\lambda$ (bit/(bit/s), i.e., s), shows the evolution time of an initial condition influencing the temperature perturbation. Therefore, it is usually used to account for the average time in which the process of temperature oscillation stability loss occurs [14,15]. Fig. 7 gives the result of the $1/\lambda$ versus the power input for T_{e4} and T_{c4} at different filling ratios. It is shown that with the increase in power input, the temperature oscillation stability loss time decrease, which is consistent with the discussion on the influence of power input on AOCT of temperature oscillations in Section 2.2.

3.4. Recurrence plots

In the analysis of time series of dynamical systems, it is often convenient to describe the system's state in phase space. Recurrence plots were introduced to simply visualize the behavior of trajectories in phase space. They are a graphic representation of the squared matrix [22]

$$R(t_i, t_j) = \Theta(\varepsilon - \|x_i - x_j\|) \quad (6)$$

where x_i stands for the point in phase space at which the system is situated at time i, ε is a predefined threshold, and $\Theta(\cdot)$ is the aforementioned Heaviside function. One assigns a "black" dot to the value one and a "white" dot to the value zero. The two dimensional graphic representation of $R_{i,j}$ then is called a recurrence plot (RP).

The RPs exhibit characteristic large scale and small scale patterns. Fig. 8 shows the recurrence plots of T_{e4} and T_{c4} at 70% filling ratio under different power inputs. A closer inspection of the RPs reveals the small scale structures which are single dots, diagonal lines (parallel to the black main diagonal line, the line of identity (LOI)) as well as vertical and horizontal lines (the combination of vertical and horizontal lines plainly forms rectangular clusters of recurrence points). In Fig. 8, the homogeneous RPs with numerous single dots and a few short diagonals indicate chaotic states [23]. To quantify these structures, the Recurrence Quantification Analysis (RQA) proposed by Webber and Zbilut [24] was used. There are different measures that can be considered in the RQA, and the distribution of the lengths of the diagonal lines $P_\varepsilon(l)$ (or $P_b(\varepsilon)$) found in a plot is a crucial point. In order to find a "black" or recurrence dot and the distribution of diagonals of length L in the RP, the probability or the rate to find such a dot is given by [23]

$$P_b(\varepsilon) = \lim_{N\to\infty} \frac{1}{N^2} \sum_{\substack{i,j=1 \\ j\neq i}}^{N} R_{i,j} \quad (7)$$

A comparison of Eqs. (3) and (7) shows the definition of $P_b(\varepsilon)$ coincides with the definition of the correlation integral $C(\varepsilon, \tau, m)$, which provides a link between the known results about the correlation integral and the structure in RPs.

The local enlarged area of the RPs with diagonal line segments of various lengths (l) is presented by Faure and Korn [25], where the correlation integral about the lengths of the diagonal lines is defined as [23]:

$$C_l(\varepsilon) = \lim_{N\to\infty} \frac{1}{N(N-1)} \sum_{i}^{N} \sum_{\substack{j=1 \\ j\neq i}}^{N} \Theta\left(\varepsilon - \left(\sum_{k=0}^{l-1} |x_{i+k} - x_{j+k}|^2\right)^{1/2}\right) \quad (8)$$

Using Eq. (8) and the G-P algorithm [26], we can obtain an estimate of the order-2 Renyi entropy K_2 [25]

$$K_2(\varepsilon, l) = \frac{1}{\tau} \ln \frac{C_l(\varepsilon)}{C_{l+1}(\varepsilon)} \quad (9)$$

Note that K_2 is a lower bound for the Kolmogorov–Sinai entropy K, and it has the same qualitative behavior of K. As an estimate of K, the value of K_2 is infinite for a random noise process, equal to zero for an ordered system, and positive for a chaotic behavior.

Based on Eq. (9), we can estimate K_2 of T_{e4} and T_{c4} from the RPs shown in Fig. 8, and the estimation results are presented in Fig. 9. At each power input, the value of K_2 of T_{e4} is larger than T_{c4} (i.e., K_2 at the evaporation section is higher than at the condensation section).The order-2 Renyi entropies of T_{e4} or T_{c4} have a trend of $K_{2,Q=87W} > K_{2,Q=60W} > K_{2,Q=37W}$, implying that the chaotic level of the temperature oscillations increasing from low power input to high power input. At other filling ratios, the order-2 Renyi entropies have the same variation trend for different power inputs. The cooperation of ever-increasing K_2 and positive, finite largest

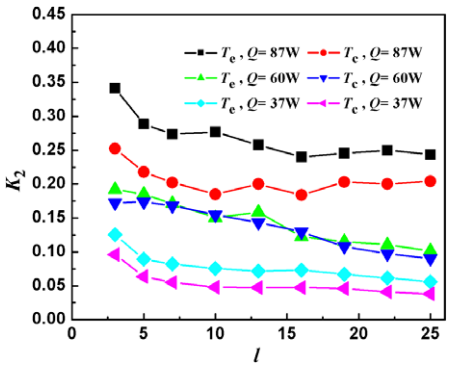

Fig. 9. K_2 of T_{e4} and T_{c4} for FR = 70% at different power inputs.

Lyapunov exponent at each filling ratio give a hint of the maximum entropy self-organization process of the temperature oscillation with the increase of the power input [27].

4. Conclusions

Temperature oscillation data at the evaporation and condensation sections of a PHP with filling ratios of 30%, 50% and 70% were obtained at three different power inputs. The data were analyzed by using non-linear analyses of the pseudo-phase-plane trajectories, the correlation dimension, the largest Lyapunov exponent and the recurrence plots. The following conclusions can be drawn from the present study:

1. The non-integer correlation dimension and its converging to a constant value as the embedding dimension increased indicating that attractors of the temperature oscillations in the PHP are strange attractors. This means that temperature oscillations are chaotic.
2. All of the positive largest Lyapunov exponents of temperature oscillations are less than 0.1, indicating the weak chaotic behavior of the PHP, instead of noise or periodic/quasi-periodic behaviors.
3. The correlation dimension increases with increasing power input indicating the increasing complexity of temperature oscillations in PHP.
4. According to the calculated correlation dimensions, the proper number of independent variables to describe the PHP operation was at least four.
5. For different power inputs (37, 60, 87 W), the correlation dimensions have a trend of $D_{E,FR=50\%} > D_{E,FR=70\%} > D_{E,FR=30\%}$. The increase of the correlation dimension from low-values to higher values leads to the enhancement of the thermal performance of a PHP. Thus, the thermal performance is the highest when the filling ratio is 50% for the three power inputs.
6. The average time of the temperature oscillation stability loss in the system decreases with the increase of the power input.
7. Chaotic states were observed in the recurrence plots of the temperature oscillations.
8. The RQA indicates that the order-2 Renyi entropies have a trend of $K_{2,Q=37W} > K_{2,Q=60W} > K_{2,Q=87W}$ at each filling ratio both for T_{e4} and T_{c4}, collaborating with the positive, finite largest Lyapunov exponent give a hint of the maximum entropy self-organization process of the temperature oscillations with the increase of the power input.

Acknowledgments

This work was supported by the National Natural Science Foundation of China through Grant No. 50536010, the Program for New Century Excellent Talents in University of China through Grant No. NCET-06-0406 and the Shanghai Municipal Education Commission through Grant Nos. 08ZZ10 and 08GG05.

References

[1] H. Akachi, US Patent No. 4921041, 1990.
[2] S. Khandekar, M. Groll, On the definition of pulsating heat pipes: an overview, in: Proceedings of 5th Minsk International Seminar (Heat pipes, Heat Pumps and Refrigerators), Minsk, Belarus, 2003, pp. 116–128.
[3] S. Khandekar, N. Dollinger, M. Groll, Understanding operational regimes of closed loop pulsating heat pipes: an experimental study, Appl. Therm. Eng. 23 (2003) 707–719.
[4] S. Khandekar, P. Charoensawan, M. Groll, P. Terdtoon, Closed loop pulsating heat pipes Part B: visualization and semi-empirical modeling, Appl. Therm. Eng. 23 (2003) 2021–2033.
[5] T.N. Wong, B.Y. Tong, S.M. Lim, K.T. Ooi, Theoretical modeling of pulsating heat pipe, Proceedings of 11th International Heat Pipe Conference, Tokyo, Japan, 1999, pp. 378–392.
[6] M.B. Shfii, A. Faghri, Y. Zhang, Thermal modeling of unlooped and looped pulsating heat pipes, J. Heat Transfer 123 (2001) 1159–1172.
[7] Y. Zhang, A. Faghri, M.B. Shafii, Analysis of liquid–vapor pulsating flow in a u-shaped miniature tube, Int. J. Heat Mass Transfer 45 (2002) 2501–2508.
[8] P. Sakulchangsatjatai, P. Chareonsawan, T. Waowaew, P. Terdtoon, M. Murakami, Mathematical modeling of closed-end pulsating heat pipes operating with a bottom heat mode, Heat Transfer Eng. 29 (2008) 238–254.
[9] W. Qu, H.B. Ma, Theoretical analysis of startup of a pulsating heat pipe, Int. J. Heat Mass Transfer 50 (2007) 2309–2316.
[10] R.T. Dobson, Theoretical and experimental modeling of an open oscillatory heat pipe including gravity, Int. J. Therm. Sci. 43 (2004) 113–119.
[11] S. Maezawa, T. Izumi, K. Gi, Experimental chaos in oscillating capillary tube heat pipes, 10th International Heat Pipe Conference, Stuttgart, German, 1997, pp. 56–61.
[12] J.L. Xu, X.M. Zhang, Start-up and steady thermal oscillation of a pulsating heat pipe, Heat Mass Transfer 41 (2005) 685–694.
[13] J.L. Xu, Y.X. Li, T.N. Wong, High speed flow visualization of a closed loop pulsating heat pipe, Int. J. Heat Mass Transfer 48 (2005) 3338–3351.
[14] R. Mosdorf, P. Cheng, H.Y. Wu, M. Shoji, Non-linear analysis of flow boiling in microchannels, Int. J. Heat Mass Transfer 48 (2005) 4667–4683.
[15] S.F. Wang, R. Mosdorf, M. Shoji, Nonlinear analysis on fluctuation feature of two-phase flow through a T-junction, Int. J. Heat Mass Transfer 46 (2003) 1519–1528.
[16] Z.J. Jiao, N.T. Nguyen, X. Huang, Chaotic motion of microplugs under high-frequency thermocapillary actuation, J. Micromech. Microeng. 17 (2007) 180–185.
[17] L.Y. Cao, Practical method for determining the minimum embedding dimension of a scalar time series, Physica D 110 (1997) 43–50.
[18] A.M. Fraaer, H.L. Swinney, Independent coordinates for strange attractors from mutual information, Phys. Rev. A 33 (1986) 1134.
[19] A. Wolf, J.B. Swift, H.L. Swinney, J.A. Vastano, Determining Lyapunov exponent from a time series, Physica D 16 (1985) 285–317.
[20] H. Kantz, A robust method to estimate the maximal Lyapunov exponent of a time series, Phys. Lett. A 185 (1994) 77.
[21] H. Kantz, T. Schreiber, Nonlinear Time Series Analysis, Cambridge University Press, Cambridge, 1997.
[22] M. Thiel, M.C. Romano, J. Kurths, How much information is contained in a recurrence plot, Phys. Lett. A 330 (2004) 343–349.
[23] M. Thiel, M.C. Romano, Estimation of dynamical invariants without embedding by recurrence plots, Chaos 14 (2004) 234–243.
[24] C.L. Webber Jr., J.P. Zbilut, Dynamical assessment of physiological systems and states using recurrence plot strategies, J. Appl. Physiol. 76 (1994) 965–973.
[25] P. Faure, H. Korn, A new method to estimate the Kolmogorov entropy from recurrence plots: its application to neuronal signals, Physica D 122 (1998) 265–279.
[26] P. Grassberger, I. Procaccia, Dimensions and entropies of strange attractors from a fluctuating dynamics approach, Physica D 13 (1984) 34–54.
[27] J.D. Phillips, Divergence, convergence, and self-organization in landscapes, Ann. Assoc. Am. Geographers 89 (1999) 466–488.